Heliyon 10 (2024) e27127

Contents lists available at ScienceDirect

Heliyon

journal homepage: www.cell.com/heliyon

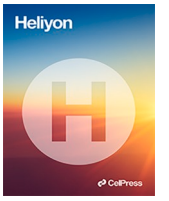

Research article

Selective recovery of metals in spent batteries by electrochemical precipitation to cathode material for sodium-ion batteries

Xiaohui Zhang [a,b,c,d], Shenglong Yang [a], Chengqing Deng [d], Wentao Liu [b], Dinghan Xiang [d], Libo Liang [a,**], Feiyan Lai [a,b,d], Kai Pan [c,*]

[a] Guangxi Hezhou Guidong Electronic Technology Co. Ltd, Hezhou, 542899, China
[b] College of Materials Science and Engineering, Guilin University of Technology, Guilin, 541004, China
[c] Institute of New Functional Materials, Guangxi Institute of Industrial Technology, Nanning, 530200, China
[d] Guangxi Key Laboratory of Information Materials, Guilin University of Electronic Technology, Guilin, 541004, China

ARTICLE INFO

Keywords:
Electrochemical separation
Metal precipitation
Recycling of spent batteries
Cathode materials
Metallic composites
Energy storage and conversion

ABSTRACT

The recycling of key components in waste lithium-ion batteries (LIBs) is an important route to make up for the shortage of battery materials. Metal separation and purification is an important step. It is of great significance to propose an efficient and green separation technology. In this paper, an electrochemical precipitation method was applied to metal separation from spent $LiNi_{0.5}Mn_{1.5}O_4$ cathode material. The Li and metal elements were effective separated and the precipitates were then used as precursor to synthesize high-performance R–O_3-NaNFM cathode material for sodium-ion batteries. The R–O_3-NaNFM exhibits excellent electrochemical cycling stability. The capacity retains 71.3 mAh g^{-1} after a long-term cycling of 200 times at 1 C. This method offers a referable strategy of the recycling for the waste cathode material in spent LIBs.

1. Introduction

Lithium-ion batteries (LIBs) are widely used in various electronic devices and electric vehicles because of superior combination performances [1]. A large number of applications of LIBs increase the pressure on upstream battery material company, and the shortage of battery materials will affect the development of the battery industry [2]. Therefore, the recycling of waste electrode materials will become the main driving force for the development of the power battery industry [3]. Waste batteries contain valuable metals and organic electrolyte, so the effective treatment of waste batteries not only to achieve the recycling of metal resources, but also to solve the caused problem of environmental pollution threatening human life [4,5]. Therefore, designing a green and low-cost recycling process has become an urgent matter. Because the cathode material contains expensive metals (Ni, Co and Li), it has become the focus among researchers [6,7].

At present, the recycling of waste cathode materials mainly includes three categories: pyrometallurgy [8,9], hydrometallurgy [10,11] and biological metallurgy [12–16]. Pyrometallurgy uses high-temperature melting to directly calcine metals in batteries into alloy compounds at high temperatures [17]. This process has the advantages of simple operation and large processing capacity. However, this method has high energy consumption, the resulting product shows low purity and a large amount of metal loss, so it has gradually

* Corresponding author.
** Corresponding author.
E-mail addresses: lianglibo321@163.com (L. Liang), pankai_09@sina.com (K. Pan).

https://doi.org/10.1016/j.heliyon.2024.e27127
Received 10 October 2023; Received in revised form 15 February 2024; Accepted 23 February 2024
Available online 24 February 2024

faded out of the researcher's vision [18]. Hydrometallurgy technology mainly leach metals from batteries with acid and alkaline reagents and then the precipitants and extraction agents selectively extract single or multiple metals. This method has gradually become a major research technology in the battery recycling industry due to its advantages of low energy consumption and high product purity [19,20]. But this technology also involves secondary pollution such as waste acid and waste alkali. Biometallurgical technology selectively leaches target metals with bacterial strains, which shows strong selectivity and high recovery rate. However, the cultivation of bacterial strains requires harsh condition and time as well as immature process [12].

Metal separation is one necessary step. The separation technology is mainly divided into solvent extraction, chemical precipitation, ion exchange, electrodeposition etc [21–24]. Solvent extraction method mainly uses extractant to selectively leach certain metal in leaching solution. Electrochemical precipitation method is mainly used to precipitate a metal by adding a chemical precipitator. Ion exchange method mainly uses ion exchange resin to selectively adsorb metals in the leaching solution, so as to achieve metal separation. These methods need certain chemical reagents which inevitably lead to secondary pollution. Electrodeposition precipitates one or several metal ions in leaching solution to achieves ion separation by controlling voltage, current and other influencing factors.

In recent years, various electrochemical pathways have been introduced into battery recycling due to their advantages of good controllability, high efficiency, simple operation, and mild conditions [25–28]. Sun et al. introduced the paired electrolysis process into the recycling field for the first time [29]. This method achieved the deposition of high-purity cobalt metal by reducing energy and reagent consumption, and left a lithium-rich solution, creating favorable conditions for further extraction of lithium. However, among the recovery technologies reported so far, there has not yet been a situation where the precursor synthesis can be achieved simultaneously during the separation process.

In this paper, the electrochemical precipitation technology is applied to the recycling of waste $LiNi_{0.5}Mn_{1.5}O_4$ (LNMO) batteries. By adjusting the voltage and current applied on the leaching solution, the Ni and Mn are precipitated in the form of oxides to realize separation from Li element. This process does not require the addition of any other chemical reagents for metal separation. In addition, the precipitate was used as precursor to prepare R–O_3-$Na[Ni_{0.3}Fe_{0.3}Mn_{0.3}]O_2$ (R–O_3-NaNFM) as cathode material of sodium-ion batteries. The electrode assembled with the regenerated R–O_3-NaNFM shows superior electrochemical performances. Fig. 1 shows a schematic diagram of recycling and regenerating processes.

2. Experimental

2.1. Leaching and electrochemical precipitation

The spent LNMO batteries (Jiangsu Chaowei New Energy Material Technology Co. Ltd.) were fully discharged in 5% NaCl solution for 24 h. Waste cathode material powder was obtained after disassembling and stripping from the cathode. The cathode material was leached in 6 mol L^{-1} HCl solution with stirring for 2 h at 80 °C.

The electrochemical precipitation was carried out in the leaching solution. In the designed separation process, the Ni and Mn elements were precipitated with Pt and Ti plates as anode and cathode respectively connected to DC power. By changing the process conditions, the pH value in the solution is continuously increased, so that the Ni and Mn elements are completely precipitated. The precipitation efficiency (ρ) of the metal ions was calculated according to Eq. (1).

$$p = [(C_1V_1–C_2V_2)/(C_1V_1)] \times 100\% \quad (1)$$

Where C_1 and C_2 (g L^{-1}) was the concentration of the metal ions in the solution tested by ICP before and after electrochemical precipitation, and V_1 and V_2 (L) was the corresponding solution volume.

The precipitation time was set for 0.5–5 h, applied voltage among 3–30 V, current density from 50 to 500 A m^{-2} at room temperature. To optimize the applicable time parameter, the applied voltage was set at 25 V. In the experiments exploring other univariate variables, the electrochemical precipitation was finished after the pH reaches 12.

Fig. 1. Schematic diagram of the recycling of the spent LNMO material to the R–O_3-NaNFM.

2.2. Preparation and characterization

The leaching solution after electrochemical precipitation was filtered to separate precipitate. Then the leaching solution containing Li^+ was filtered and concentrated to be evolved into the crystallized lithium salt. A certain amount of $Ni(CH_3COO)_2$ and $Fe(CH_3COO)_2$ was added into the obtained precipitate to match the molar ratio of Ni: Fe: Mn = 1: 1: 1. The mixture and the Na_2CO_3 were mixed evenly and calcined at 480 °C for 5 h and 900 °C for 10 h in succession under O_2 flow. The synthesized cathode material is labeled as R–O_3-NaNFM. The comparison sample of O_3–$Na[Ni_{0.3}Fe_{0.3}Mn_{0.3}]O_2$ (O_3-NaNFM) was synthesized using $Ni(CH_3COO)_2$, $Fe(CH_3COO)_2$ and Na_2CO_3 as raw materials in stoichiometric ratio through the same preparation process. The crystalline structure was characterized by X-ray diffraction (XRD, Rigaku, D/Max-2500 V/PC, Tokyo, Japan) equipped with Cu Kα radiation (k = 0.15406 nm). The morphology and detailed lattice spacing was observed by scanning electron microscope (SEM, Philips, FEI Quanta 200 FEG) equipped with energy dispersive spectrometer (EDS) for elemental analysis. The X-ray photoelectron spectroscopy (XPS, Thermo Scientific, Escalab 250 XI) was carried out to analyze the valence state based on the surface compositions.

2.3. Electrochemical testing

The cathode material was prepared with the O_3-NaNFM and R–O_3-NaNFM materials, super P (SP) and polyvinylidene fluoride (PVDF) (weight ratio was 8: 1: 1) solved in N-methyl-2-pyrrolidone (NMP). The slurry mixture was coated on Al foil as a current collecting agent, and vacuum dried at 80 °C for 12 h to obtain a cathode sheet, and a sodium sheet was used as counter electrode. The electrolyte was 1.0 M $NaClO_4$ in ethylene carbonate (EC) and diethyl carbonate (DEC) (1:1 by volume) with 8 vol% fluoroethylene carbonate (FEC) additive, the cell was assembled in an Ar-filled glovebox. The galvanostatic charge and discharge test was carried out at 25 °C between 2.5 and 4.3 V on a battery tester (LAND CT2001A, China). The electrochemical impedance spectroscopy (EIS) was tested at the IM6 electrochemical workstation (Zahner-Elektrik GmbH & Co. KG, Germany) with a frequency range from 0.01 to 100 kHz.

3. Results and discussion

Fig. 2a shows the effect of electrolysis time on the precipitation rate of Ni and Mn. It can be seen that the precipitation efficiency of the two metals increases with the increase of electrolysis time. When the electrolysis time reaches to 4 min, the precipitation rate of the two metals is close to 100%. In order to explore the mechanism of metal precipitation, the pH value during the electrolysis process was studied. The change of pH value with electrolysis time is shown in Fig. 2b. When the electrolysis time is 5 h, the pH value is 12 which reaches the K_{sp} value of Ni and Mn precipitation. When the voltage is 25 V, the precipitation rates of Mn and Ni reaches 99.1% and 99.5% respectively (Fig. 2c). When the current density reaches 300 A m^{-2}, the leaching rate of Ni and Mn is close to 100% (Fig. 2d). Under the optimal conditions (electrolysis time of 5 h, voltage of 25 V, and current density of 300 A m^{-2}), the Ni and Mn ions can be

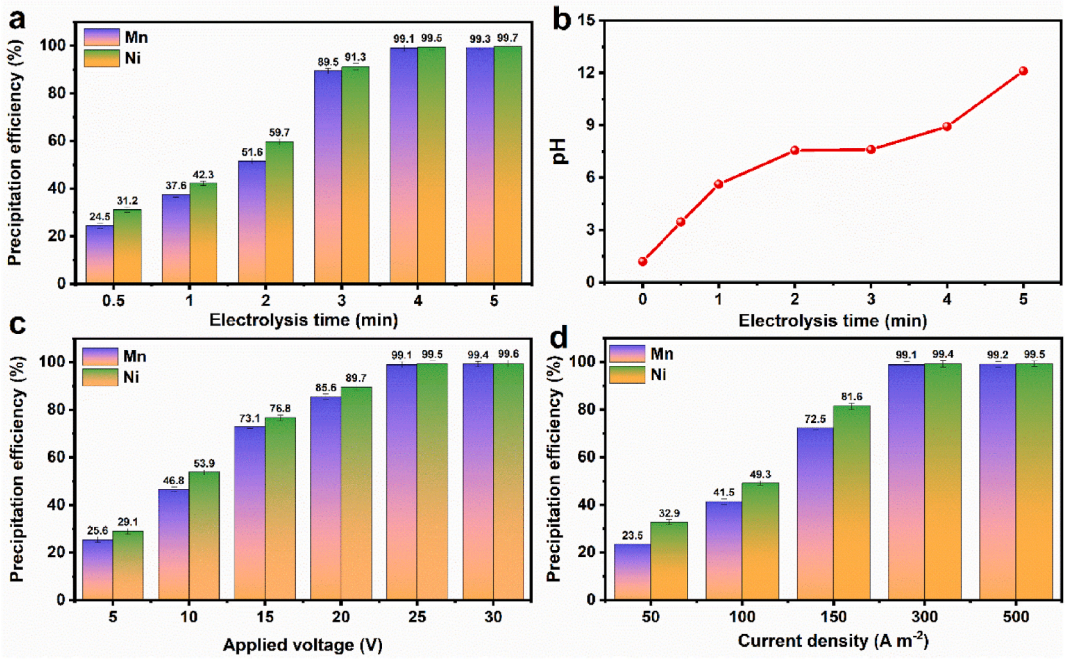

Fig. 2. Precipitation efficiency of metal ions at different electrolysis conditions: electrolysis time (a), electrolysis time on pH value in solution (b), applied voltage (c), current density (d).

completely precipitated at room temperature to achieve the purpose of metal separation and Li elements in the leach solution.

Fig. 3a–b shows SEM image of the sediment. The sediment shows uniformly dispersed particles, which is conducive to uniform mixing with sodium salt. The smaller particle size can effectively improve the rate capability of the electrode. (Fig. 3c–d). This uniform size particle is due to the uniformity of the precursor particles (Fig. 3e–f). The uniformity of particle is even better than the commercial O_3-NaNFM. Fig. 3g shows XRD pattern of the O_3-NaNFM, the sharp peaks are consistent with the standard card of O_3-NaNFM (PDF#54–0887) and no impurity peaks appear in the pattern. The peaks of the R–O_3-NaNFM at 19°and 44° are related to the formation of Na_2CO_3 due to the degradation of the O_3-layered structure in ambient condition. The strong diffraction peaks reveal that the material has a good crystal structure. The same valence state and peak position appear for the both materials. The C 1s spectra shows the presence of C–C (284.6 eV), C–O (285.1 eV), and CO_3^{2-} (288.6 eV), mainly attribute to residual Na_2CO_3 (Fig. 3h) [30]. This is mainly attributed to the excessive sodium salt added to the two materials, so some carbonate remains on the surface. Fig. 3i shows the main peak of Mn 2p which is divided into four peaks attributed to the characteristic peaks of Mn^{3+} (641.8 and 653.8 eV) and Mn^{4+} (642.6 and 652.8 eV), respectively. Fig. 3j shows the main peak of Ni 2p divided into four peaks at 854.9, 856.2, 871.8 and 872.1 eV, which are attributed to the characteristic peaks of Ni^{2+} and Ni^{3+}, respectively. The O 1s spectra mainly be attribute to the O^{2-} in the crystal lattice (529.4 and 531.2 eV) and the deposited oxygen on the surface (532.6 eV) of the particles. Meanwhile the peaks at 535.6 eV can be ascribed to the electrolyte oxidation (Fig. 3k). Fig. 3l shows the main peak of Fe 2p, the peaks at 711.1 and 726.1 eV correspond to the Fe^{3+} [31].

Fig. 4a–b shows CV curves of the O_3-NaNFM and R–O_3-NaNFM electrodes in SIBs. Both curves have the same peak location and two pairs of redox peaks. The polarization difference of the R–O_3-NaNFM is close to that of the O_3-NaNFM. As illustrated in Fig. 4c, the discharge/charge curves of the two materials at a current density of 0.1C are in the potential window of 2.0–4.3 V. The initial discharge/charge capacities are 166.89/184.5 mAh g^{-1} and 160.1/181.2 mAh g^{-1}, respectively, corresponding to initial coulombic efficiency of 90.46% and 88.36%. The first coulomb efficiency of the R–O_3-NaNFM materials is slightly lower than that of the O_3-NaNFM. The R–O_3-NaNFM electrode delivers 162.5 and 83.8 mAh g^{-1} at the current densities of 0.2C and 10 C (Fig. 4d). The capacity of the R–O_3-NaNFM at 10 C rate is lower than that of the O_3-NaNFM. This may be due to the larger particles of the recycled materials affects the migration path of ions. This phenomenon is more obvious under high-rate charge and discharge currents. The capacity comes back to the initial value as current density returns to 0.2C. Meanwhile, the material still exhibits a high charge capacity of 83.8 mAh g^{-1} at a high rate of 10 C. Fig. 4e shows the electrode is cycled after 200 times at 1 C. The repeated insertion of Na^+ cause structure collapse and sodium deficiency will occur on cathode under long cycling. Moreover, the decomposition of the electrolyte also lead to the degradation of capacity. The capacity still reaches 71.3 mAh g^{-1}, which is comparable to the O_3-NaNFM (75.6 mAh g^{-1}).

Fig. 5a–b shows the Nyquist plots of the O_3-NaNFM and R–O_3-NaNFM. The curves of both electrodes are composed of a semicircles in high-frequency region and an oblique lines in low-frequency region. The high-frequency region represents the interface resistance, and the low-frequency region represents the charge transfer resistance. It can be seen that the resistance of the O_3-NaNFM is lower than that of the R–O_3-NaNFM. Due to the instantaneous rise of pH value to the K_{sp} of Ni and Mn during electrolysis, the produced precipitate

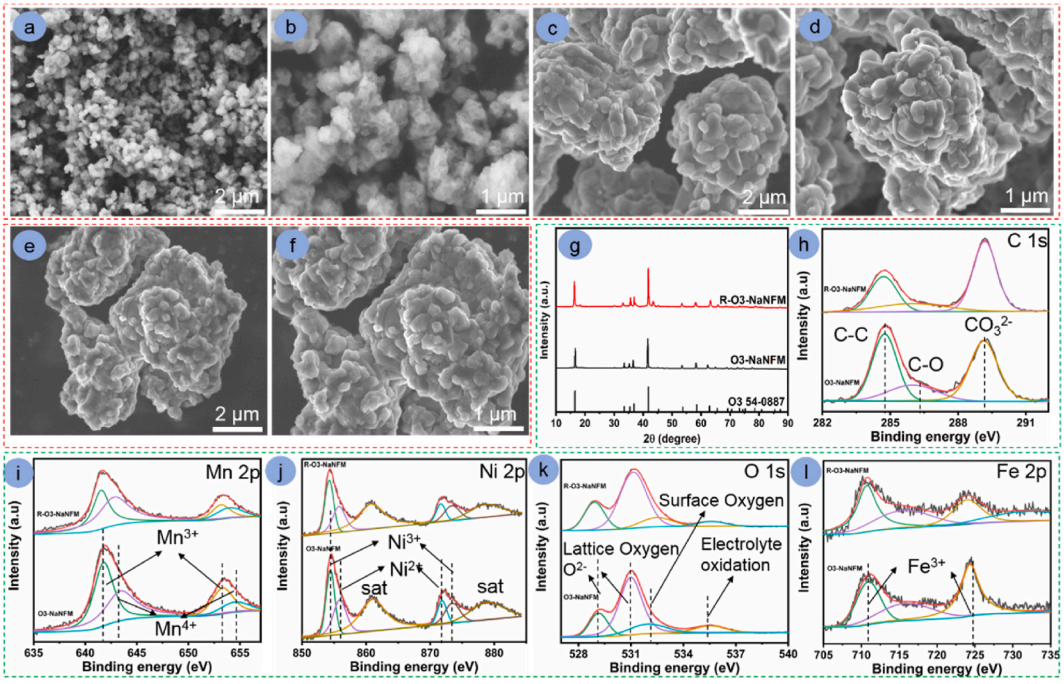

Fig. 3. SEM of the precipitate (a, b), O_3-NaNFM (c, d) and R–O_3-NaNFM (e, f), XRD pattern (g) and XPS spectra of the O_3-NaNFM and R–O_3-NaNFM: C 1s (h), Mn 2p (i), Ni 2p (j), O 1s (k) and Fe 2p (l).

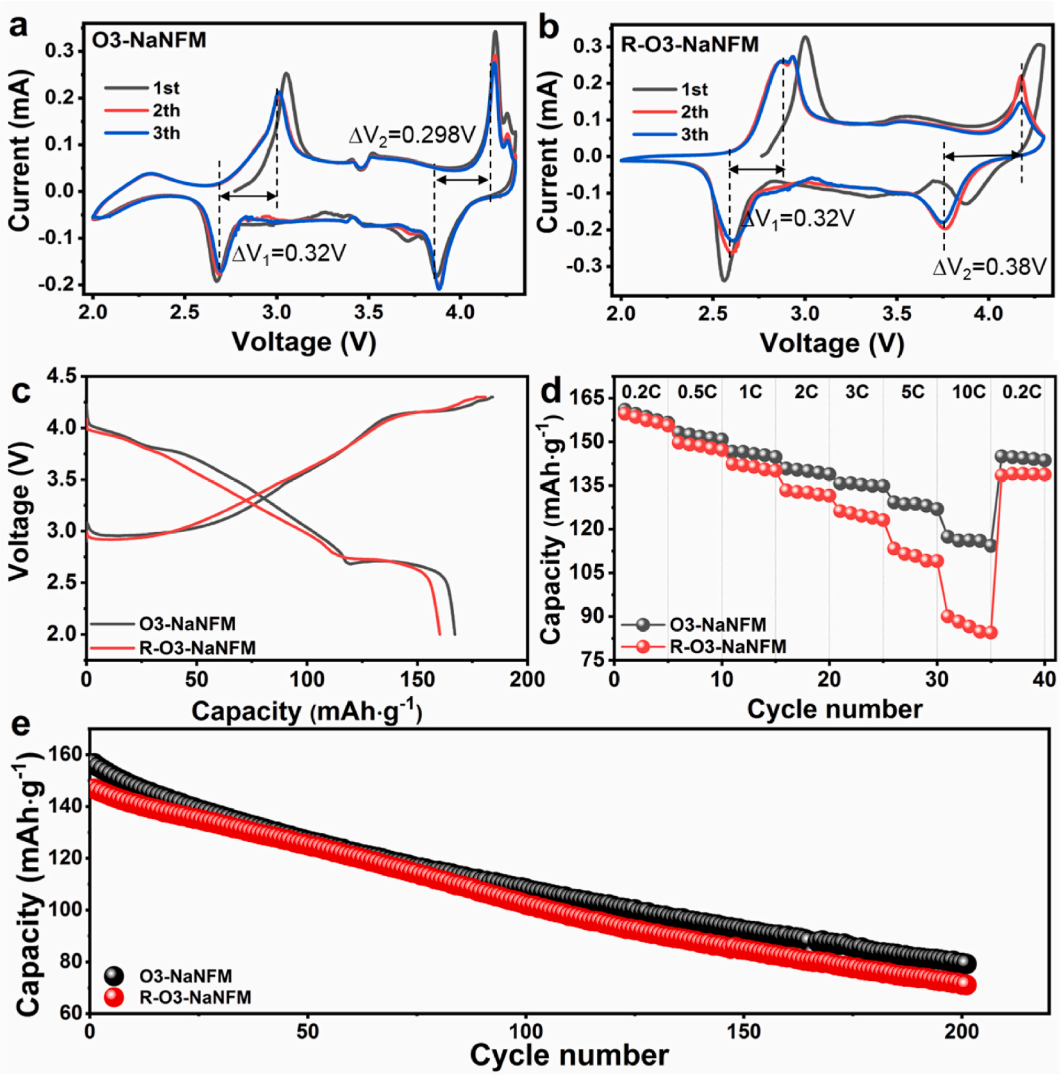

Fig. 4. CV of the O_3-NaNFM (a) and R–O_3-NaNFM (b), the initial discharge/charge profiles (c), rate capability (d) and cycling performance (e) of the O_3-NaNFM and R–O_3-NaNFM.

show larger particle size increasing charge transfer impedance. And the poor consistency of the particle size and morphology also increases interface resistance of the cathode material obtained by electrolysis. The table in Fig. 5c shows the fitted calculation result of the O_3-NaNFM and R–O_3-NaNFM, it is further proved that the resistance of the O_3-NaNFM electrode is smaller than that of the R–O_3-NaNFM. The results correspond to the magnification diagram in Fig. 4d.

Fig. 6a–b shows the TEM images of the two materials after cycling. The crystal lattice changes slightly, which may be the reason for the capacity decay of the two materials. The degree of lattice deformation of the R–O_3-NaNFM is greater than that of the O_3-NaNFM. These factors can affect the electrochemical performances.

4. Conclusion

In this paper, an electrochemical precipitation method is used in the recycling of waste LIBs. The Ni and Mn were precipitated in form of oxides to realize separation with Li element without any other chemical reagents. Under optimal conditions, the precipitation rate of Ni and Mn is close to 100%. The precursor of the R–O_3-NaNFM as cathode material of SIBs was successfully prepared while the metal separation was realized in the leaching solution of the metals. The prepared R–O_3-NaNFM material has an electrochemical property comparable to the commercial sample. The assembled electrode shows a capacity of up to 71.3 mAh g^{-1} after 200 times at 1 C. This work provides a new opportunity and reference for the recycling of waste LIBs.

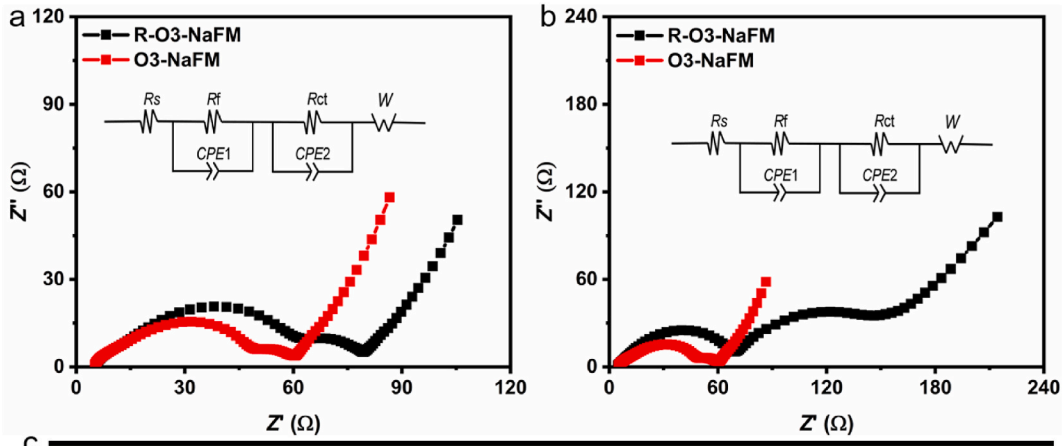

c

Sample	Impedance value					
	4 th			50 th		
	R_s	R_{sf}	R_{ct}	R_s	R_{sf}	R_{ct}
R-O_3-NaNFM	5.88	11.73	4.53	5.08	92.64	68.83
O_3-NaNFM	5.04	3.38	3.74	4.78	52.08	33.72

Fig. 5. Nyquist plots of the O_3-NaNFM (a) and R–O_3-NaNFM (b), results through fitting calculation (c) of O_3-NaNFM and R–O_3-NaNFM.

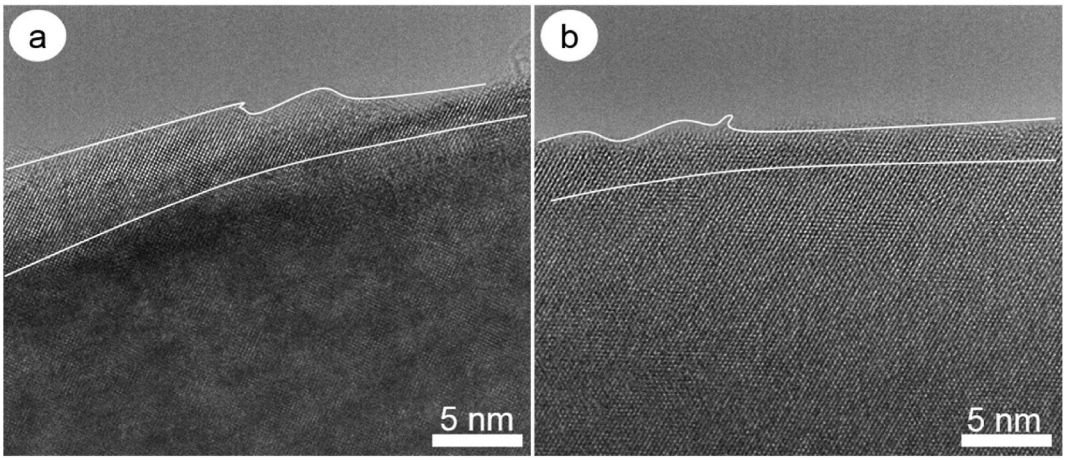

Fig. 6. TEM images of the R–O_3-NaNFM (a) and O_3-NaNFM (b).

CRediT authorship contribution statement

Xiaohui Zhang: Writing – original draft. **Shenglong Yang:** Methodology. **Chengqing Deng:** Methodology. **Wentao Liu:** Resources. **Dinghan Xiang:** Resources, Data curation. **Libo Liang:** Supervision. **Feiyan Lai:** Formal analysis. **Kai Pan:** Writing – review & editing.

Declaration of competing interest

The authors declare that they have no known competing financial interests or personal relationships that could have appeared to influence the work reported in this paper.

Acknowledgments

This research was supported by National Natural Science Foundation (51964013), Guangxi Natural Science Foundation (2022GXNSFAA035610), Specific Research Project for Research Bases and Talents of Guangxi (GUIKE AD23026038), Guangxi Key Research and Development Project (GUIKE AB21196006), Hezhou Science Research and Technology Development Program (2021ZX31288), Guangxi Key Laboratory of Information Materials (Guilin University of Electronic Technology), P.R. China (221003-K).

References

[1] F. Arshad, L. Li, K. Amin, E. Fan, N. Manurkar, A. Ahmad, J. Yang, F. Wu, R. Chen, A comprehensive review of the advancement in recycling the anode and electrolyte from spent lithium ion batteries, ACS Sustain. Chem. Eng. 8 (36) (2020) 13527–13554.
[2] M. Chen, X. Ma, B. Chen, R. Arsenault, P. Karlson, N. Simon, Y. Wang, Recycling end-of-life electric vehicle lithium-ion batteries, Joule 3 (11) (2019) 2622–2646.
[3] Abhishek Sarkar, Pranav Shrotriya, C. Ikenna, Nlebedim, Electrochemical-driven green recovery of lithium, graphite and cathode from lithium-ion batteries using water, Waste Manage. (Tucson, Ariz.) 150 (2022) 320–327.
[4] J.B. Dunn, L. Gaines, J. Sullivan, M. Wang, Impact of recycling on cradle-to-gate energy consumption and greenhouse gas emissions of automotive lithium-ion batteries, Environ. Sci. Technol. 46 (22) (2012) 12704–12710.
[5] Y. Bai, N. Muralidharan, Y. Sun, S. Passerini, M. Stanley Whittingham, I. Belharouak, Energy and environmental aspects in recycling lithium-ion batteries: concept of battery identity global passport, Mater. Today 41 (2020) 304–315.
[6] S. Natarajan, V. Aravindan, Recycling strategies for spent Li-ion battery mixed cathodes, ACS Energy Lett. 3 (9) (2018) 2101–2103.
[7] C. Vaalma, D. Buchholz, M. Weil, S. Passerini, Electrolytes for stable and safer sodium-based batteries, Nat. Rev. Mater. 3 (2018) 18013.
[8] M. Zhou, Pyrometallurgical technology in the recycling of a spent lithium ion battery: evolution and the challenge, ACS ES&T Eng. 1 (10) (2021) 1369–1382.
[9] T. Georgi-Maschler, B. Friedrich, R. Weyhe, H. Heegn, M. Rutz, Development of a recycling process for Li-ion batteries, J. Power Sources 207 (2012) 173–182.
[10] X. Chen, J. Li, D. Kang, T. Zhou, H. Ma, A novel closed-loop process for the simultaneous recovery of valuable metals and iron from a mixed type of spent lithium-ion batteries, Green Chem. 21 (23) (2019) 6342–6352.
[11] S.P. Barik, G. Prabaharan, L. Kumar, Leaching and separation of Co and Mn from electrode materials of spent lithium-ion batteries using hydrochloric acid: Laboratory and pilot scale study, J. Clean. Prod. 147 (2017) 37–43.
[12] J. Li, G. Wang, Z. Xu, Environmentally-friendly oxygen-free roasting/wet magnetic separation technology for in situ recycling cobalt, lithium carbonate and graphite from spent $LiCoO_2$/graphite lithium batteries, J. Hazard Mater. 302 (2016) 97–104.
[13] N. Vieceli, R. Casasola, G. Lombardo, B. Ebin, M. Petranikova, Hydrometallurgical recycling of EV lithium-ion batteries: effects of incineration on the leaching efficiency of metals using sulfuric acid, Waste Manage. (Tucson, Ariz.) 125 (2021) 192–203.
[14] P. Liu, L. Xiao, Y. Tang, Y. Chen, L. Ye, Y. Zhu, Study on the reduction roasting of spent $LiNi_xCo_yMn_zO_2$ lithium-ion battery cathode materials, J. Therm. Anal. Calorim. 136 (2019) 1323–1332.
[15] J. Lin, L. Li, E. Fan, C. Liu, X. Zhang, H. Cao, Z. Sun, R. Chen, Conversion mechanisms of selective extraction of lithium from spent lithium-ion batteries by sulfation roasting, ACS Appl. Mater. Interfaces 12 (16) (2020) 18482–18489.
[16] J. Lin, C. Liu, H. Cao, R. Chen, Y. Yang, L. Li, Z. Sun, Environmentally benign process for selective recovery of valuable metals from spent lithium-ion batteries by using conventional sulfation roasting, Green Chem. 21 (2019) 5904–5913.
[17] K. Meng, Y. Cao, B. Zhang, X. Ou, D. Li, J. Zhang, X. Ji, Comparison of the ammoniacal leaching behavior of layered $LiNi_xCo_yMn_{1-x-y}O_2$ (x = 1/3, 0.5, 0.8) cathode materials, ACS Sustain. Chem. Eng. 7 (8) (2019) 7750–7759.
[18] Y. Ma, J. Tang, R. Wanaldi, X. Zhou, H. Wang, C. Zhou, J. Yang, A promising selective recovery process of valuable metals from spent lithium ion batteries via reduction roasting and ammonia leaching, J. Hazard Mater. 402 (2021) 123491–1234101.
[19] R. Ciez, J. Whitacre, Examining different recycling processes for lithium-ion batteries, Nat. Sustain. 2 (2019) 148–156.
[20] W. Lv, Z. Wang, H. Cao, Y. Sun, Y. Zhang, Z. Sun, A critical review and analysis on the recycling of spent lithium-ion batteries, ACS Sustainable Chem. Eng. 6 (2) (2018) 1504–1521.
[21] H. Li, S. Xing, Y. Liu, F. Li, H. Guo, G. Kuang, Recovery of lithium, iron, and phosphorus from spent LiFePO4 batteries using stoichiometric sulfuric acid leaching system, ACS Sustain. Chem. Eng. 5 (9) (2017) 8017–8024.
[22] E. Fan, L. Li, X. Zhang, Y. Bian, Q. Xue, J. Wu, F. Wu, R. Chen, Selective recovery of Li and Fe from spent lithium-ion batteries by an environmentally friendly mechanochemical approach, ACS Sustain. Chem. Eng. 6 (8) (2018) 11029–11035.
[23] D. Pant, D. Joshi, M. Upreti, R. Kotnala, Chemical and biological extraction of metals present in E waste: a hybrid technology, Waste Manage. (Tucson, Ariz.) 32 (5) (2012) 979–990.
[24] S. Joo, S. Shin, D. Shin, C. Oh, J. Wang, Extractive separation studies of manganese from spent lithium battery leachate using mixture of PC88A and Versatic 10 acid in kerosene, Hydrometallurgy 156 (2015) 136–141.
[25] K. Liu, S. Yang, F. Lai, H. Wang, Y. Huang, F. Zheng, S. Wang, X. Zhang, Q. Li, Innovative electrochemical strategy to recovery of cathode and efficient lithium leaching from spent lithium-ion batteries, ACS Appl. Energy Mater. 3 (5) (2020) 4767–4776.
[26] H. Shuai, J. Li, W. Hong, X. Gao, G. Zou, J. Hu, H. Hou, X. Ji, H. Liu, Electrochemically modulated $LiNi_{1/3}Mn_{1/3}Co_{1/3}O_2$ cathodes for lithium-ion batteries, Small Methods 3 (5) (2019) 1900065.
[27] B. Zhang, X. Qu, J. Qu, X. Chen, H. Xie, P. Xing, D. Wang, H. Yin, A paired electrolysis approach for recycling spent lithium iron phosphate batteries in an undivided molten salt cell, Green Chem. 22 (2020) 8633–8641.
[28] H. Lv, H. Huang, C. Huang, Q. Gao, Z. Yang, W. Zhang, Electric field driven de-lithiation: a strategy towards comprehensive and efficient recycling of electrode materials from spent lithium ion batteries, Appl. Catal. B Environ. 283 (2021) 119634.
[29] W. Lv, D. Ruan, X. Zheng, L. Li, H. Cao, Z. Wang, Y. Zhang, Z. Sun, One-step recovery of valuable metals from spent Lithium-ion batteries and synthesis of persulfate through paired electrolysis, Chem. Eng. J. 421 (1) (2021) 129908.
[30] H. Wang, F. Ding, Y. Wang, X. Rong, L. Zhang, Y. Hu, In situ plastic-crystal-coated cathode toward high-performance Na-ion batteries, ACS Energy Lett. 8 (3) (2023) 1434–1444.
[31] T. Wei, X. Liu, S. Yang, P. Wang, T. Yi, Regulating the electrochemical activity of Fe-Mn-Cu-based layer oxides as cathode materials for high-performance Na-ion battery, J. Energy Chem. 80 (2023) 603–613.